Causal Viscous Hydrodynamics for Central Heavy-Ion Collisions

Rudolf Baier[1] and Paul Romatschke[2]

[1]*Fakultät für Physik, Universität Bielefeld, D-33501 Bielefeld, Germany*
[2]*Institute for Nuclear Theory, University of Washington, Box 351550, Seattle WA, 98195, USA*
(Dated: February 5, 2008)

We study causal viscous hydrodynamics in the context of central relativistic heavy-ion collisions and provide details of a straightforward numerical algorithm to solve the hydrodynamic equations. It is shown that correlation functions of fluctuations provide stringent test cases for any such numerical algorithm. Passing these tests, we study the effects of viscosity on the temperature profile in central heavy-ion collisions. Also, we find that it is possible to counter-act the effects of viscosity to some extent by re-adjusting the initial conditions. However, viscous corrections are strongest for high-mass particles, signaling the breakdown of hydrodynamic descriptions for large η/s.

I. INTRODUCTION

Successful fits of ideal hydrodynamics to experimental data on several observables [1, 2, 3, 4, 5] at the highest energies of the ongoing heavy-ion program [6, 7, 8, 9] at the Relativistic Heavy-Ion Collider (RHIC) seem to indicate a very small value of the ratio shear viscosity over entropy. Since calculations of this ratio in QCD at weak coupling $\alpha_s \ll 1$ give [10, 11] a numerical value that turns out to be larger by about one order of magnitude than the conjectured strong coupling value for relativistic quantum field theories at finite temperature [12] (see also [13]), this has given rise to the idea of a "strongly-coupled" quark-gluon plasma phase [14, 15, 16, 17, 18, 19, 20].

However, up to now calculations in the regime of strong coupling are limited to theories which possess a gravity dual theory, such as $\mathcal{N} = 4$ Super Yang-Mills Theory [21]. So far, no such dual theory has been discovered for QCD, meaning that the main available tool to study dynamical processes in QCD are based on weak-coupling approaches (although lattice-based techniques for making quantitative measurements of near-equilibrium quantities may be available soon [22, 23]).

Given that the numerical value of the QCD coupling α_s within the range of temperatures applicable for RHIC is assumed to be close to the range $\alpha_s = 0.2 - 0.4$, one observes that while this value is not very small, it is not very large either. Thus, although it would be of great interest to have results for QCD at very strong coupling, there is at least some hope that existing weak-coupling techniques might actually offer a description of RHIC physics that is not inferior to still-to-be-discovered QCD strong-coupling techniques (or likewise, extrapolating existing strong-coupling results from theories (very) different than QCD).

Along these lines, it has recently been discovered that non-Abelian plasma instabilities [24] create turbulent color magnetic fields [25, 26] that may induce a very small effective ("anomalous") shear viscosity coefficient [27, 28], without invoking strong coupling effects. Within the initial conditions obtained in the color-glass-condensate model [29] it is, however, unclear whether this effect is relevant for present RHIC energies [30, 31].

Regardless of these issues, it is important to note that so far the ratio of shear viscosity over entropy density for RHIC energies is fairly unconstrained. While the general trend of viscous corrections to ideal hydrodynamics has been studied by Teaney [32], a dynamical implementation of viscous hydrodynamics and comparison to experimental data is still lacking. This is partly due to the fact that the "simplest" form of viscous hydrodynamics, the relativistic Navier-Stokes equations, are be-riddled by acausality problems and instabilities [33]. Therefore, there has been recent interest in so-called second-order (Israel-Stewart[34]) theories [35, 36, 37, 38, 39, 40, 41, 42] which are, however, of more complicated structure than the Navier-Stokes equations.

Specifically, it seems that adapting existing numerical hydrodynamic solvers to treat Israel-Stewart theory for all but the simplest geometries is a non-trivial task. It might therefore be worthwhile to devise completely new algorithms that are more suitable (or at least simpler) than present hydrodynamic solvers. Along these lines, in this work we present a straightforward algorithm for solving Israel-Stewart viscous hydrodynamic equations for geometries that are longitudinally expanding, are space-time rapidity independent and have radial symmetry and thus should be well suited to describe viscous hydrodynamics of central collisions at RHIC and in the future at the Large Hadron Collider (LHC).

Our work is organized as follows: in section II we review the equations of causal viscous hydrodynamics and present evidence that our numerical algorithm reproduces the ideal hydrodynamic behavior in the limit of a small ratio of viscosity over entropy, as it should.

In section III, we present a more involved test that is based on measuring correlation functions of small fluctuations and comparing to analytic results.

In section IV, our results for the temperature evolution and particle spectra in relativistic causal viscous hydrodynamics are presented and we give our conclusions in section V.

II.   SETUP AND COMPARISON WITH IDEAL HYDRODYNAMICS

The basic equations of causal viscous hydrodynamics that we choose to study are given by [39]

$$(\epsilon + p)Du^\mu = \nabla^\mu p - \Delta^\mu_\nu \nabla_\sigma \Pi^{\nu\sigma} + \Pi^{\mu\nu} Du_\nu \,, \tag{1}$$

$$D\epsilon = -(\epsilon + p)\nabla_\mu u^\mu + \frac{1}{2}\Pi^{\mu\nu}\langle \nabla_\nu u_\mu \rangle \,, \tag{2}$$

$$\tau_\Pi \Delta^\mu_\alpha \Delta^\nu_\beta D\Pi^{\alpha\beta} + \Pi^{\mu\nu} = \eta \langle \nabla^\mu u^\nu \rangle - 2\tau_\Pi \Pi^{\alpha(\mu} \omega^{\nu)}_\alpha \,, \tag{3}$$

where ϵ, p are the energy density and pressure, respectively, u^μ is the flow four-velocity that obeys $u_\mu u^\mu = 1$ and $\Pi^{\mu\nu}$ is the shear tensor that fulfills $u_\mu \Pi^{\mu\nu} = 0 = \Pi^\mu_\mu$ and characterizes the viscous deviations in the energy momentum tensor,

$$T^{\mu\nu} = (\epsilon + p)u^\mu u^\nu - pg^{\mu\nu} + \Pi^{\mu\nu}. \tag{4}$$

Furthermore, η and τ_Π are the shear viscosity coefficient and relaxation time that are related by $\frac{\eta}{\tau_\Pi} = \frac{2p}{3}$ in weakly-coupled QCD [39] and the remaining definitions are

$$d_\mu u^\nu \equiv \partial_\mu u^\nu + \Gamma^\nu_{\alpha\mu} u^\alpha, \qquad D \equiv u_\mu d^\mu, \qquad \nabla^\mu \equiv \Delta^{\mu\nu} d_\nu,$$

$$\Delta^{\mu\nu} \equiv g^{\mu\nu} - u^\mu u^\nu, \qquad \omega^{\mu\nu} = \Delta^{\mu\alpha}\Delta^{\nu\beta}\frac{1}{2}\left(d_\beta u_\alpha - d_\alpha u_\beta\right),$$

$$\langle A_\mu B_\nu \rangle \equiv A_\mu B_\nu + A_\nu B_\mu - \frac{2}{3}\Delta_{\mu\nu}A_\alpha B^\alpha, \qquad (A_\mu, B_\nu) \equiv \frac{1}{2}\left(A_\mu B_\nu + A_\nu B_\mu\right), \tag{5}$$

where $\Gamma^\nu_{\alpha\mu}$ are the Christoffel symbols. As outlined in the introduction, we will be interested in systems which are rapidity-invariant and have radial symmetry, therefore we choose to work in co-moving and radial coordinates τ, r, ϕ, η with the relations $\tau = \sqrt{t^2 - z^2}$, $r^2 = x^2 + y^2$, $\tan\phi = y/x$ and $\eta = \mathrm{atanh}(z/t)$. The only non-vanishing fluid velocity components are then u^τ and u^r with the relation $u^\tau = \sqrt{1 + (u^r)^2}$ and neglecting gradients in ϕ and η we find for the above equations

$$(\epsilon + p)Du^\tau = \left(1 - (u^\tau)^2\right)\left(\partial_\tau p - d_\nu \Pi^\nu_\tau\right) - u^\tau u^r \left(\partial_r p - d_\nu \Pi^\nu_r\right)$$

$$(\epsilon + p)Du^r = -u^\tau u^r \left(\partial_\tau p - d_\nu \Pi^\nu_\tau\right) - \left(1 + (u^r)^2\right)\left(\partial_r p - d_\nu \Pi^\nu_r\right)$$

$$D\epsilon = -(\epsilon + p)\theta + \frac{1}{2}\left(-\Pi^r_r(1 - v^2)^2\langle\nabla^r u^r\rangle - r^2\,\Pi^\phi_\phi\langle\nabla^\phi u^\phi\rangle - \tau^2\,\Pi^\eta_\eta\langle\nabla^\eta u^\eta\rangle\right)$$

$$-d_\nu \Pi^\nu_\tau = v^2 \partial_\tau \Pi^r_r + v \partial_r \Pi^r_r + \Pi^r_r \left(\partial_\tau v^2 + \partial_r v + \frac{v^2}{\tau} + \frac{v}{r} \right) + \frac{1}{\tau} \Pi^\eta_\eta$$

$$d_\nu \Pi^\nu_r = v \, \partial_\tau \Pi^r_r + \partial_r \Pi^r_r + \Pi^r_r \left(\partial_\tau v + \frac{v}{\tau} + \frac{2 - v^2}{r} \right) + \frac{1}{r} \Pi^\eta_\eta$$

$$\tau_\Pi D \Pi^\eta_\eta + \Pi^\eta_\eta = -\eta \, \tau^2 \, \langle \nabla^\eta u^\eta \rangle$$

$$\tau_\Pi D \Pi^r_r + \Pi^r_r = -\eta \, \langle \nabla^r u^r \rangle + 2 u^r \tau_\Pi \left(\Pi^r_\tau D u^\tau + \Pi^r_r D u^r \right)$$

$$\langle \nabla^r u^r \rangle = -2 \partial_r u^r - 2 u^r D u^r + \tfrac{2}{3} \left(1 + (u^r)^2 \right) \theta, \qquad r^2 \langle \nabla^\phi u^\phi \rangle = -2 \frac{u^r}{r} + \tfrac{2}{3} \theta,$$

$$\tau^2 \langle \nabla^\eta u^\eta \rangle = -2 \frac{u^\tau}{\tau} + \tfrac{2}{3} \theta, \qquad \theta = \partial_\tau u^\tau + \partial_r u^r + \frac{u^\tau}{\tau} + \frac{u^r}{r} \tag{6}$$

where $v = u^r / u^\tau$, $\Pi^r_\tau = -v \, \Pi^r_r$, $\Pi^\phi_\phi = -\Pi^\eta_\eta - (1 - v^2) \Pi^r_r$ and here $D = u^\tau \partial_\tau + u^r \partial_r$. This system of equations has to be closed by providing an equation of state, e.g. $\epsilon = \epsilon(p)$.

Clearly, it is possible to use the relation $u^\tau = \sqrt{1 + (u^r)^2}$ to eliminate either u^τ or u^r from the above equations. Defining $\gamma = u^\tau = (1 - v^2)^{-1/2}$ one obtains

$$\left[\gamma^4 (\epsilon + p) - (1 - v^2 \gamma^2) \Pi^r_r \right] \partial_\tau v = -\gamma^2 (\partial_r + v \partial_\tau) p + (\partial_r + v \partial_\tau) \Pi^r_r - \left[\gamma^4 v (\epsilon + p) + \gamma^2 v \Pi^r_r \right] \partial_r v$$

$$+ \left(\frac{v}{\tau} + \frac{2}{r} \right) \Pi^r_r - \gamma^2 \left(\frac{v}{\tau} - \frac{1}{r} \right) \Pi^\eta_\eta$$

$$\partial_\tau \epsilon = - \left[(\epsilon + p) \gamma^2 - \Pi^r_r \right] v \partial_\tau v - v \partial_r \epsilon - (\epsilon + p) \left[\gamma^2 \partial_r v + \frac{1}{\tau} + \frac{v}{r} \right]$$

$$+ \Pi^r_r \left[\partial_r v - \frac{v}{\gamma^2 r} \right] - \Pi^\eta_\eta \left[\frac{v}{r} - \frac{1}{\tau} \right]. \tag{7}$$

However, in the code we prefer to keep both u^τ and u^r, solving equations for them independently so that a non-trivial consistency check on the numerics is provided by monitoring the deviation of $(u^\tau)^2 - (u^r)^2$ from unity.

A. Discretization

We use discretized space-time and compute differentials of a function $f(\tau, r)$ as finite differences,

$$\partial_r f(\tau, r) = \frac{f(\tau, r + a) - f(\tau, r - a)}{2a}, \qquad \partial_\tau f(\tau, r) = \frac{f(\tau + \delta\tau, r) - f(\tau, r)}{\delta\tau}, \tag{8}$$

where $a, \delta\tau$ are the spatial and temporal lattice spacings, respectively. The boundaries are taken care of by using one-sided derivatives.

Provided a starting condition at time $\tau = \tau_0$ for the variables $u^\tau, u^r, \epsilon, \Pi^r_r, \Pi^\eta_\eta$ one can then integrate the set of equations (6) forward in time. The virtue of this approach is that one immediately obtains the results for the fluid velocities etc. rather than having to perform the "usual" hydrodynamic algorithm (transforming to the calculational frame, integrating equations, transforming back). The drawback is that in Eqs. (6), time derivatives of the above variables are still coupled (e.g. the first equation of Eqs. (6) contains both $\partial_\tau u^\tau$ and $\partial_\tau p$). However, since all time derivatives enter only linearly this can be rectified by making use of a linear equation solver so that e.g. $\partial_\tau u^\tau = f(\tau, r)$ which can be directly integrated using the above discretization.

In practice, this works as follows: from the first equation in Eqs.(6) we pick out the coefficients of the time derivatives $\partial_\tau u^\tau, \partial_\tau u^r, \partial_\tau p$ and label them as a_{00}, a_{01}, a_{02}, respectively. The remaining part of the equation, which contains no time derivative, is called b_0. Thus, it becomes of the form

$$a_{00} \partial_\tau u^\tau + a_{01} \partial_\tau u^r + a_{02} \partial_\tau p = b_0. \tag{9}$$

Note that in order to obtain this form we have expanded out the derivatives $d_\nu \Pi^\nu_\tau, d_\nu \Pi^\nu_r$ by using the relevant equations in (6). A similar procedure for the second and third equation of (6) leaves us with

$$
\begin{aligned}
a_{10}\partial_\tau u^\tau + a_{11}\partial_\tau u^r + a_{12}\partial_\tau p &= b_1 \\
a_{20}\partial_\tau u^\tau + a_{21}\partial_\tau u^r + a_{22}\partial_\tau p &= b_2.
\end{aligned}
\tag{10}
$$

With $\delta_j = \partial_\tau(u^\tau, u^r, p)$, these three equations may be written in matrix form as $a_{ij}\delta_j = b_i$, which has a solution unless $\det a_{ij} = 0$. Numerically, this matrix equation is readily solved using a standard linear-equations solver, so δ_j is known explicitly and may be used to finally compute $\partial_\tau \Pi^\eta_\eta$ and $\partial_\tau \Pi^r_r$. This completes the setup of our algorithm[1].

B. Testing the Code – Ideal Hydrodynamics

As a first test, we run our numerical code for a very small value of viscosity, $\eta/s = 10^{-4}$ and compare our results to ideal hydrodynamics. Our problem of choice is to start with a configuration for the energy density

$$
\epsilon(r, \tau_0) = \frac{\epsilon_0}{1 + \exp\left[(r - R)/\sigma\right]},
\tag{11}
$$

where $R = 6.4$ fm can be thought of as the "radius" of a nucleus, and ϵ_0 is such that the temperature (assuming an ideal gluon gas) is $T_0 = 0.2$ GeV at $r = 0$. The parameter σ is in principle arbitrary, but we choose it to be $\sigma = 0.02$ fm in order to have a very steep fall of the energy density near $r \simeq R$. Choosing the ideal equation of state $\epsilon(p) = 3p$ for which the speed of sound squared $c_s^2 = \frac{1}{3}$, we can then compare the time evolution of temperature and velocity to the analytic solution

$$
\begin{aligned}
T_{\text{Baym}}(r, \tau) &= T_0 e^{-c_s \alpha_R(r, \tau - \tau_0)} \left(\frac{\tau_0}{\tau}\right)^{c_s^2\left[1 + (1 - c_s v_R(r, \tau - \tau_0))^{-1}\right]/2} \\
v_{\text{Baym}}(r, \tau) &= \tanh\left[\alpha_R(r, \tau - \tau_0) + \frac{c_s^2}{2}\left(\frac{v_R(r, \tau - \tau_0)}{1 - c_s v_R(r, \tau - \tau_0)}\right)\ln\left(\frac{\tau - \tau_0}{\tau_0}\right)\right] \\
\alpha_R(r, t) &= \begin{cases} 0 &: \quad r < R - c_s t \\ -\frac{1}{2}\ln\left(\frac{t - r + R}{t + r - R}\frac{1 - c_s}{1 + c_s}\right) &: \quad R - c_s t < r < R + t \\ \infty &: \quad r > R + t \end{cases} \\
v_R(r, t) &= \begin{cases} 0 &: \quad r < R - c_s t \\ \frac{r - R + c_s t}{t + c_s(r - R)} &: \quad R - c_s t < r < R + t \\ 1 &: \quad r > R + t \end{cases}
\end{aligned}
\tag{12}
$$

from Baym et al. [46]. Results are shown in Fig.1, where it can be seen that – within the errors of the approximate analytic solution – the numerical solution agrees with the results Eq.(12).

III. FLUCTUATIONS AND LINEARIZED VISCOUS HYDRODYNAMICS

Motivated by cosmology where one can actually observe correlations of density fluctuations in the early universe [43, 44, 45], we study radial fluctuations of the energy density ϵ, the flow velocity

---

[1] A version of the code, written in reasonably well documented C, may be obtained upon request from paulrom@physik.uni-bielefeld.de
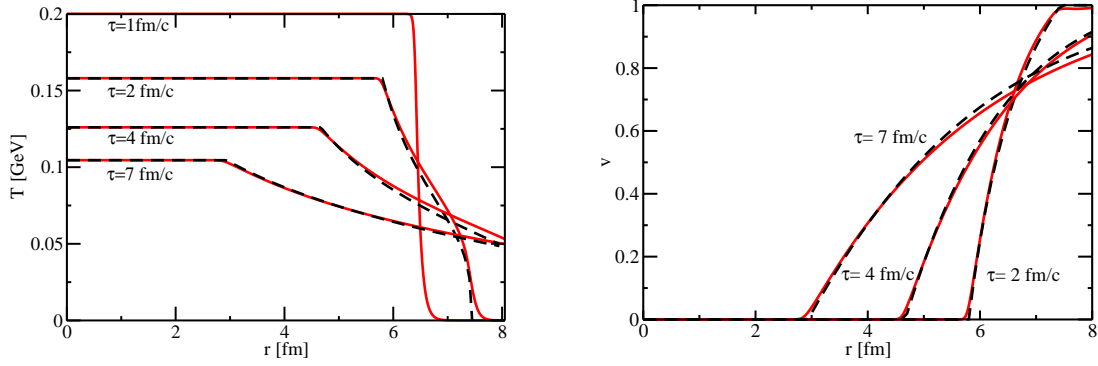
FIG. 1: Comparison between numerical results and the analytic approximation Eq.(12) (full and dashed lines, respectively) for the evolution of the temperature (left figure) and the velocity $v = \frac{u^r}{u^\tau}$ (right figure). The slight disagreement between numerical and analytical results is due to the approximations involved in the analytic solution and has the same sign and size as in the original work [46].

v and the shear tensor $\Pi^{\mu\nu}$ around a background solution $\epsilon_0, u_0^r, \Pi_0^{\mu\nu}$ such that

$$\epsilon(\tau, r) = \epsilon_0(\tau) + \delta\epsilon(\tau, r), \qquad v(\tau, r) = \delta v(\tau, r), \qquad \Pi^{\mu\nu} = \Pi_0^{\mu\nu}(\tau) + \delta\Pi^{\mu\nu}(\tau, r) \qquad (13)$$

where the background solution obeys the equations [36, 47]

$$\partial_\tau \epsilon_0 = -\frac{\epsilon_0 + p_0}{\tau} + \frac{1}{\tau}\Pi^\eta_{\eta, 0} \qquad \partial_\tau \Pi^\eta_{\eta, 0} = -\frac{1}{\tau_\Pi}\Pi^\eta_{\eta, 0} + \frac{8p_0}{9\tau} \qquad (14)$$

and we remind that $\frac{\eta}{\tau_\Pi} = \frac{2p_0}{3}$.

In what follows, we will assume that the fluctuations around the background are small so we keep only terms linear in the perturbations ("linearized hydrodynamics", c.f. [48, 49]). Note, however, that we keep the full non-trivial time dependence of the background, which to the best of our knowledge has not been done before in the context of heavy-ion collisions even in the case of ideal hydrodynamics.

To slightly simplify the discussion, we want to assume in this section that τ_Π is constant with respect to time (which consequently requires a time-dependent ratio of η/s), whereas in other sections of this work τ_Π will be time-dependent. To linear order in the perturbations one is thus left with the set of coupled partial differential equations

$$\left[(\epsilon_0 + p_0 - \Pi^r_{r,0})\partial_\tau + c_s^2\partial_\tau\epsilon_0 - \left(\partial_\tau + \frac{1}{\tau}\right)\Pi^r_{r,0} + \frac{1}{\tau}\Pi^\eta_{\eta,0}\right]\delta v + c_s^2\partial_r\delta\epsilon - \left[\partial_r + \frac{2}{r}\right]\delta\Pi^r_r - \frac{1}{r}\delta\Pi^\eta_\eta = 0$$

$$\left[(\epsilon_0 + p_0)\left(\partial_r + \frac{1}{r}\right) - \Pi^r_{r,0}\left(\partial_r - \frac{1}{r}\right) + \frac{1}{r}\Pi^\eta_{\eta,0}\right]\delta v + \left[\partial_\tau + \frac{1 + c_s^2}{\tau}\right]\delta\epsilon - \frac{1}{\tau}\delta\Pi^\eta_\eta = 0$$

$$\frac{4}{9}p_0\left[\partial_r + \frac{1}{r}\right]\delta v - \frac{8}{9}\frac{c_s^2}{\tau}\delta\epsilon + \left[\partial_\tau + \frac{1}{\tau_\Pi}\right]\delta\Pi^\eta_\eta = 0$$

$$\frac{4}{9}p_0\left[-2\partial_r + \frac{1}{r}\right]\delta v + \frac{4}{9}\frac{c_s^2}{\tau}\delta\epsilon + \left[\partial_\tau + \frac{1}{\tau_\Pi}\right]\delta\Pi^r_r = 0. \quad (15)$$

These can be further simplified by noting that for the initial condition $\Pi_0^{\mu\nu} = 0$ and no radial flow one has $\Pi^r_{r,0} = \Pi^\phi_{\phi,0}$ and as a consequence of $\Pi^\mu_{\mu,0} = 0$ the relation $\Pi^r_{r,0} = -\frac{1}{2}\Pi^\eta_{\eta,0}$ holds for all τ.

Usually one would do a space-like Fourier transform to get rid of the space-like derivatives. Due to our choice of coordinates, however, this is obviously not possible. However, upon introducing

$$\delta\bar{\Pi} = \left(\partial_r + \frac{2}{r}\right)\delta\Pi_r^r + \frac{1}{r}\delta\Pi_\eta^\eta \qquad (16)$$

we can achieve the same goal by doing a so-called Bessel-Fourier transform,

$$\delta v(\tau, r) = \int_0^\infty d\kappa J_1(\kappa r)\delta\tilde{v}(\tau,\kappa), \qquad \delta\epsilon(\tau,r) = \int_0^\infty d\kappa J_0(\kappa r)\delta\tilde{\epsilon}(\tau,\kappa),$$
$$\delta\bar{\Pi}(\tau,r) = \int_0^\infty d\kappa J_1(\kappa r)\delta\tilde{\Pi}(\tau,\kappa), \qquad \delta\Pi_\eta^\eta(\tau,r) = \int_0^\infty d\kappa J_0(\kappa r)\delta\tilde{\Pi}_\eta^\eta(\tau,\kappa) \ , \qquad (17)$$

where the property of the Bessel functions J_n

$$\int_0^\infty dr\, r J_n(\kappa r)J_n(\kappa' r) = \frac{\delta(\kappa - \kappa')}{\kappa} \qquad (18)$$

can be used to invert the above transformations. Using an ideal equation of state, $p_0 = c_s^2\epsilon_0$ and the Eqs. (14) to remove explicit time derivatives on ϵ_0 and $\Pi_{\eta,0}^\eta$ we thus find

$$\left[(\epsilon_0 + p_0 + \frac{1}{2}\Pi_{\eta,0}^\eta)\partial_\tau + c_s^2\partial_\tau\epsilon_0 + \frac{1}{2}\left(\partial_\tau + \frac{3}{\tau}\right)\Pi_{\eta,0}^\eta\right]\delta\tilde{v} - \kappa c_s^2\delta\tilde{\epsilon} - \delta\tilde{\Pi} = 0$$

$$\left[\epsilon_0 + p_0 + \frac{1}{2}\Pi_{\eta,0}^\eta\right]\kappa\delta\tilde{v} + \left[\partial_\tau + \frac{1+c_s^2}{\tau}\right]\delta\tilde{\epsilon} - \frac{1}{\tau}\delta\tilde{\Pi}_\eta^\eta = 0$$

$$\frac{4}{9}p_0\kappa\delta\tilde{v} - \frac{8}{9}\frac{c_s^2}{\tau}\delta\tilde{\epsilon} + \left[\partial_\tau + \frac{1}{\tau_\Pi}\right]\delta\tilde{\Pi}_\eta^\eta = 0$$

$$\frac{8}{9}p_0\kappa^2\delta\tilde{v} - \frac{4}{9}\kappa\frac{c_s^2}{\tau}\delta\tilde{\epsilon} + \left[\partial_\tau + \frac{1}{\tau_\Pi}\right]\delta\tilde{\Pi} = 0. \qquad (19)$$

A. Sonic peaks in Ideal Hydrodynamics

Upon first taking the limit $\tau_\Pi \to 0$ and then setting $\Pi_0^{\mu\nu}$ as well as $\delta\Pi^{\mu\nu}$ to zero we recover the equations for fluctuations in ideal hydrodynamics, which together with $\epsilon_0 \propto \tau^{-1-c_s^2}$ require

$$\left[\partial_\tau^2 - \frac{c_s^2}{\tau}\partial_\tau + \frac{c_s^2}{\tau^2} + c_s^2\kappa^2\right]\delta\tilde{v}(\tau,\kappa) = 0 \qquad (20)$$

(and a similar differential equation for $\delta\tilde{\epsilon}$). As can be quickly verified, the solutions to the linearized ideal hydrodynamic equations then become

$$\delta v(\tau, r) = \int_0^\infty d\kappa J_1(\kappa r)\tau^{(1+c_s^2)/2}\left[A(\kappa)\, J_{(-1+c_s^2)/2}(\kappa c_s\tau) + B(\kappa)\, Y_{(-1+c_s^2)/2}(\kappa c_s\tau)\right],$$

$$\frac{\delta\epsilon(\tau, r)}{\epsilon_0(\tau)} = -\frac{1+c_s^2}{c_s}\int_0^\infty d\kappa J_0(\kappa r)\tau^{(1+c_s^2)/2}\left[A(\kappa)\, J_{(1+c_s^2)/2}(\kappa c_s\tau) + B(\kappa)\, Y_{(1+c_s^2)/2}(\kappa c_s\tau)\right], \quad (21)$$

where J and Y are both Bessel functions of the first kind and A, B are constants of integration.

As initial conditions at the starting time $\tau = \tau_0$ we choose for simplicity $\delta v(\tau_0, r) = 0$ and random noise for $\delta\epsilon(\tau_0, r)$ with a correlation function [2]

$$\epsilon_0^{-2} < \delta\epsilon(\tau_0, r)\, \delta\epsilon(\tau_0, r') >= \Delta^2\frac{\delta(r - r')}{r}, \qquad (22)$$

---

[2] Let $f^{(i)}(r)$ be the ith configuration of an observable f. The correlation function $< f(r)f(r') >$ is then defined as $< f(r)f(r') >\equiv \lim_{N\to\infty}\frac{1}{N}\sum_{i=1}^N f^{(i)}(r)f^{(i)}(r')$.

which is the polar-coordinate equivalent of a Gaussian distribution with standard deviation Δ.

This initial condition has the advantage that it implies

$$< A(\kappa)A(\kappa') >= \kappa\delta(\kappa-\kappa')\frac{\Delta^2 c_s^2}{\tau_0^{1+c_s^2}(1+c_s^2)^2}\left[J_{(1+c_s^2)/2}(\kappa c_s\tau_0) - Y_{(1+c_s^2)/2}(\kappa c_s\tau_0)\frac{J_{(-1+c_s^2)/2}(\kappa c_s\tau_0)}{Y_{(-1+c_s^2)/2}(\kappa c_s\tau_0)}\right]^{-2}, \tag{23}$$

such that

$$\epsilon_0^{-2}(\tau) < \delta\epsilon(\tau,r)\,\delta\epsilon(\tau,r') >= \int_0^\infty d\kappa\,\kappa\,J_0(\kappa r)J_0(\kappa r')f(\kappa,\tau,\tau_0) \tag{24}$$

where

$$f(\kappa,\tau,\tau_0) = \left(\frac{\tau}{\tau_0}\right)^{1+c_s^2}\Delta^2\frac{\left[J_{(1+c_s^2)/2}(\kappa c_s\tau)Y_{(-1+c_s^2)/2}(\kappa c_s\tau_0) - Y_{(1+c_s^2)/2}(\kappa c_s\tau)J_{(-1+c_s^2)/2}(\kappa c_s\tau_0)\right]^2}{\left[J_{(1+c_s^2)/2}(\kappa c_s\tau_0)Y_{(-1+c_s^2)/2}(\kappa c_s\tau_0) - Y_{(1+c_s^2)/2}(\kappa c_s\tau_0)J_{(-1+c_s^2)/2}(\kappa c_s\tau_0)\right]^2}. \tag{25}$$

Despite its ugly appearance, this is a nice result since for large κ we find

$$f(\kappa,\tau,\tau_0) \to \left(\frac{\tau}{\tau_0}\right)^{c_s^2}\Delta^2\cos^2\left(\kappa c_s(\tau - \tau_0)\right), \tag{26}$$

which are just the sonic peaks that one can also derive in cosmology.

This result can serve as a stringent test on the numerical algorithm used to solve the hydrodynamic equations as the position of the maxima and minima of f as a function of κ are very sensitive to the speed of sound. In what follows, we thus initialize our numerical algorithm with precisely the same initial conditions as discussed above and then measure the correlation function $\epsilon_0^{-2}(\tau) < \delta\epsilon(\tau,r)\,\delta\epsilon(\tau,r') >$ to extract $f(\kappa,\tau,\tau_0)$ by using Eq.(18) to integrate out[3] both r,r',

$$\int_0^\infty r\,dr\int_0^\infty r'\,dr'J_0(\kappa r)J_0(\kappa' r')\epsilon_0^{-2}(\tau) < \delta\epsilon(\tau,r)\,\delta\epsilon(\tau,r') >= \frac{\delta(\kappa - \kappa')}{\kappa}f(\kappa,\tau,\tau_0). \tag{27}$$

To maximize the signal, we pick $\kappa = \kappa'$ which is regular on the lattice we use to solve the hydrodynamic equations.

In Fig.2 we show the result for[4] $f(\kappa,\tau,\tau_0)$ obtained on a lattice with lattice spacing $a = 0.25$ GeV^{-1} and $N = 8192$ sites and $\eta/s = 10^{-4}$, ensemble-averaged over 100 configurations and coarse grained in κ, for three different times τ. Up to three sonic peaks can be nicely distinguished and the comparison with the analytic result Eq.(25) indicates that our code indeed accurately solves the ideal hydrodynamic equations with the "correct" speed of sound. There is, however, a slight discrepancy between the numerical measured correlation function and its analytic result at small κ and later times: presumably, this is due to the fact that on the lattice, only a finite number of momenta can be simulated and thus the inversion formula Eq.(27) holds only approximately. Indeed, the second part of Fig.2 shows that this discrepancy can be systematically reduced by going to larger lattice volumes. Since the solution of the viscous hydrodynamic equations themselves do not depend on relations such as Eq.(27), this discrepancy should not be mistaken as a failure of the algorithm to correctly treat low momentum modes.

---

[3] Since we solve the hydrodynamic equations on a lattice, in practice we do the integrations by summing over all lattice sites. Furthermore, momenta $\kappa = \frac{\pi k}{Na}$ are also discrete, where a is the spatial lattice spacing, N the number of lattice sites and k is a positive integer smaller than $N/2$.

[4] Note that the lattice dispersion relation $\kappa = a^{-1}\sin(\pi k/N)$ has been used to convert to continuum values.
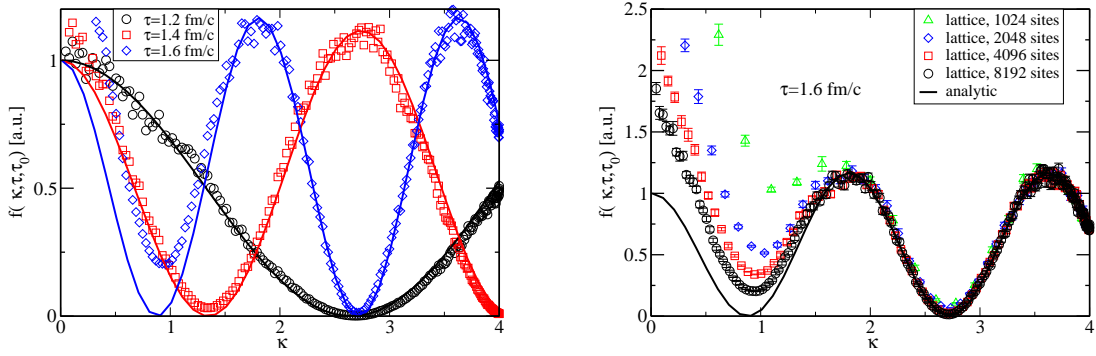
FIG. 2: Left figure: The correlation function $f(\kappa, \tau, \tau_0)$ from solving hydrodynamic equations on a lattice (symbols, see text for details) for $\tau_0 = 1$ fm/c and different τ compared to the analytic result (full lines). As one can see, the agreement between the analytic result and the measured correlation function is very good in general (a slight difference e.g. in the speed of sound would be clearly visible by a shift in the minima/maxima of f). Note that at later times, a discrepancy at low momenta κ develops. This is probably a lattice artifact since increasing the simulated volume reduces the discrepancy (right figure).

B. Sonic Peaks in Viscous Hydrodynamics

Treating the set of equations (19) in their full generality we were unable to find analytic solutions like those obtained in the previous subsection. However, since together with Eq.(14) these are just a set of six coupled ordinary differential equations they readily lend themselves to numerical solutions, which we nevertheless want to refer to as "analytic" since they are completely independent of our numerical algorithm to solve the hydrodynamic equations.

With the same initial conditions as in the previous subsection one therefore obtains an "analytic" solution of the correlation function $f(\kappa, \tau, \tau_0)$, with both expansion and viscosity included. In Fig.3, this "analytic" solution is again compared to the correlation function obtained by solving the hydrodynamic equations on a lattice (for $\eta/s = 0.1$ and $\eta/s = 0.3$, respectively). Similarly to the case of vanishing viscosity, we find that there is very good general agreement between the measured (ensemble averaged and coarse-grained) correlation function and the "analytic" result, except for later times and small momenta κ, where lattice artifacts seem to be accumulating.

Since also in this case the position and width of the sonic peaks are very sensitive to the value of η/s and the speed of sound, we argue that the good agreement between measured and "analytic" correlation functions is a strong indication that our numerical code is indeed correctly solving the second order viscous hydrodynamic equations.

Finally, we want to point out that fluctuation measurements may also help to constrain the value of η/s from RHIC data, as has been recently suggested [50].

IV. CAUSAL VISCOUS HYDRODYNAMICS WITH TRANSVERSE FLOW

Let us now study the effects of viscosity on quantities of interest for heavy-ion collisions. For simplicity, we will assume that the radial energy density profile is given by Eq.(11), where we take $R_0 = 6.4$ fm and $\sigma = 0.54$ fm which has been used before for ideal hydrodynamic calculations [46]. The constant e_0 is chosen such that we have an initial temperature T_0 at $r = 0$. In accordance with ideal hydrodynamic studies in their simplest form we assume that at the time when we start
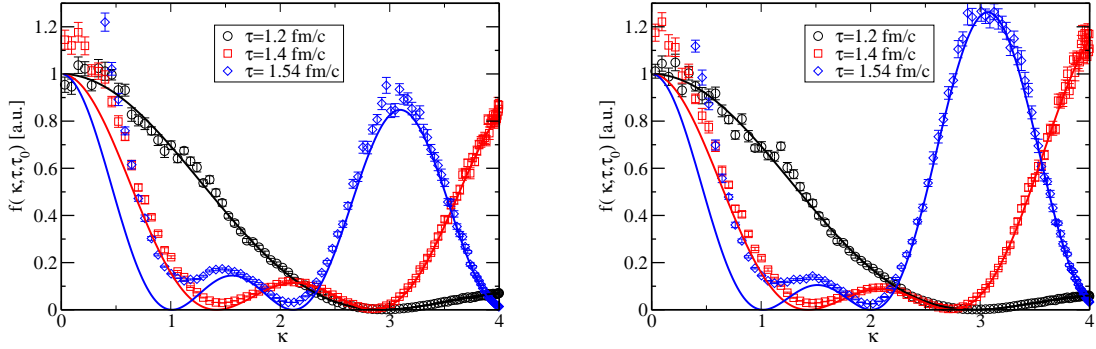
FIG. 3: Comparison for $f(\kappa, \tau, \tau_0)$ from solving hydrodynamic equations on a lattice (symbols, $\eta/s = 0.1$ (left) and $\eta/s = 0.3$ (right), respectively) with 4096 sites and lattice spacing $a = 0.25 \, \text{GeV}^{-1}$ and "analytic" solution (full lines) of Eqs.(19).

applying our hydrodynamic description ($\tau = \tau_0$), the system does not have any transverse flow already, so $v = 0$. Furthermore, since this is still an exploratory study, we pick a simplistic equation of state, $p = c_s^2 \epsilon$ with constant speed of sound $c_s^2 = 1/3$.

This set of initial conditions would be sufficient to determine the subsequent dynamics fully in the case of ideal hydrodynamics. Including the effects of viscosity requires that we pick a specific value of the ratio η/s and also provide initial conditions for the two independent components of $\Pi^{\mu\nu}$ at $\tau = \tau_0$. Maybe the simplest choice would be to assume – like in ideal hydrodynamics – that the system for some reason happens to be in equilibrium at $\tau = \tau_0$, such that "accidentally" $\Pi^{\mu\nu} = 0$. This choice probably highlights best the difference of viscous hydrodynamics to ideal hydrodynamics, since one starts from the same initial condition, so we will use it as our initial condition in the following.

However, there are other "sensible" choices of initial conditions that might be more relevant for real heavy-ion collisions in the future. E.g. within the Color-Glass-Condensate model in its simplest form (the McLerran-Venugopalan model [51]), the system does not have any longitudinal dynamics, so after times $\tau > Q_s^{-1}$ where Q_s is the saturation scale, the system essentially has zero longitudinal pressure [52, 53]. In the local rest frame $u^r = u^\phi = u^\eta = 0$, so with $c_s^2 = 1/3$, Eq.(4) would imply

$$\Pi^\eta_\eta = p, \quad \Pi^r_r = -\frac{p}{2} \tag{28}$$

Finally, going beyond the McLerran-Venugopalan model to include so called next-to-leading order corrections of gluon production [54, 55] one has to take into account the effect of rapidity fluctuations and full three-dimensional gauge field dynamics. This has recently been shown to trigger instabilities [30], leading to the generation of non-zero longitudinal pressure [56] at $\tau > Q_s^{-1}$. Pending the result using the correct rapidity fluctuation spectrum [57], the initial condition for $\Pi^{\mu\nu}$ is expected to lie somewhere in-between the two cases discussed above.

A. Temperature Profile in Viscous Hydrodynamics

Choosing the initial condition $\Pi^{\mu\nu} = 0$ at $\tau = \tau_0$, we can investigate the changes of the temperature profile from the ideal hydrodynamic behavior due to dynamical viscous effects. In Fig.4 we show the temperature as a function of the radius for $T_0 = 0.36$ GeV at $\tau_0 = 1$ fm/c, but
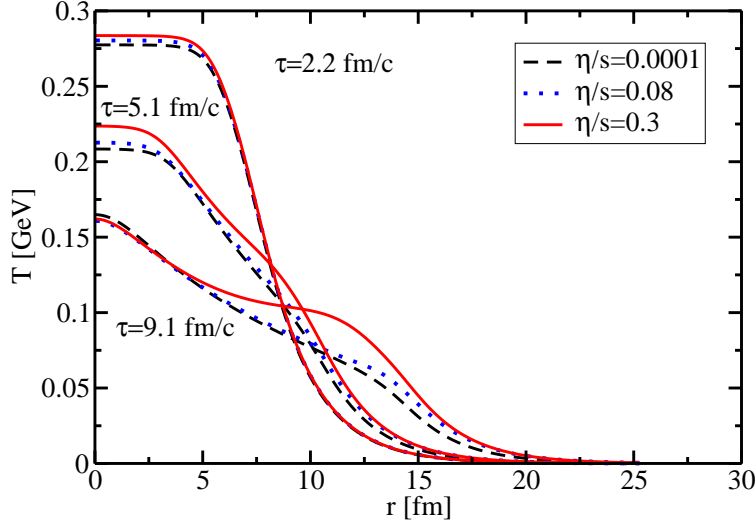
FIG. 4: Temperature profile for calculations with different η/s (dashed, dotted and solid lines, respectively) for three different times (see text for details). As expected, for larger values of η/s, differences to ideal hydrodynamics are biggest and viscous hydrodynamics initially cools slower than ideal hydrodynamics. However, note that in certain regions and at later times, viscous hydrodynamics turns out to give temperatures slightly smaller than the corresponding ideal hydrodynamic calculation.

different values of η/s, calculated on a lattice with 512 sites and $a = 0.25$ GeV^{-1} lattice spacing. Choosing the temporal time step as $\delta\tau = 0.005a$ we find that the violation $\sqrt{|(u^\tau)^2 - (u^r)^2 - 1|}$, summed over all lattice sites and divided by the number of sites always stays smaller than one percent, providing yet another check on the numerics. Finally, we have checked that choosing $a = 1$ or 0.5 GeV^{-1} does not result in any noticeable deviations of our calculated temperature profile, thus we have some confidence that our results are not strongly affected by numerical artifacts.

For early times, the behavior shown in Fig.4 shows that – as in the case of neglecting transverse flow [36, 39] – in viscous hydrodynamics the temperature decreases slower than in ideal hydrodynamics. However, at late times this behavior is seemingly counteracted by viscous radial dynamics: at very small values of the radius, the viscous hydrodynamic equations result in slightly lower temperatures than in the ideal hydrodynamic case. Note that such behavior has been also found in [58, 59].

B. Particle Spectra in Viscous Hydrodynamics

The success of the hydrodynamic picture in the context of heavy-ion collision builds upon the ability to fit the particle spectra observed in these collisions. While now methods of how to convert hydrodynamic quantities such as energy density and fluid velocity into particle spectra have reached some sophistication, the main building block still seems to involve the Cooper-Frye freeze-out prescription [60] in some form or the other, which states that the spectrum of particles with energy E and momentum p is given by

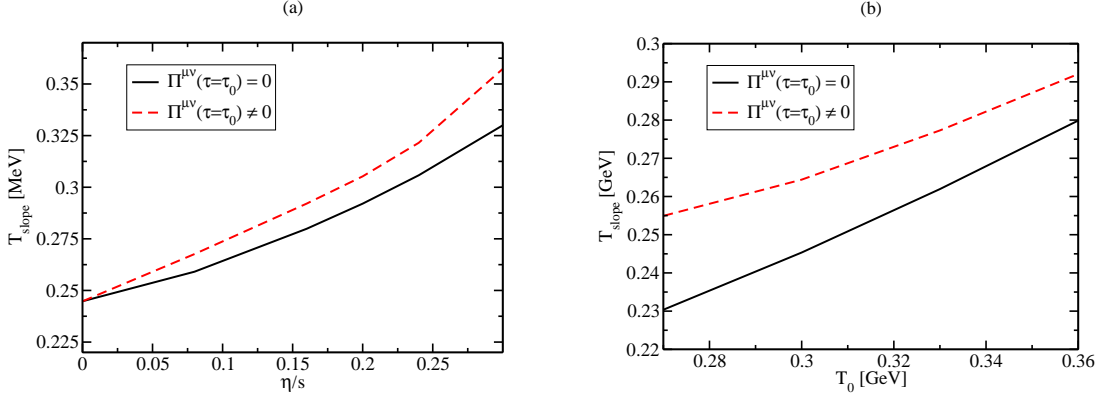$$E\frac{d^3N}{d^3p} = \frac{d}{(2\pi)^3} \int p_\mu d\Sigma^\mu f\left(\frac{p_\mu u^\mu}{T}\right),$$ (29)

FIG. 5: Inverse slope parameter T_{slope} for $T_f = 0.135$ GeV and $\tau_0 = 1$ fm/c. Two initial conditions for $\Pi^{\mu\nu}$, corresponding to pressure isotropy (full line) and vanishing longitudinal pressure (dashed line) at $\tau = \tau_0$ are shown. Choosing $T_0 = 0.36$ GeV (left), the spectra become increasingly flatter when raising η/s, while this effect can be compensated by lowering T_0 (right, shown for $\eta/s = 0.16$).

where d is the degeneracy of the particles and u^μ is the velocity which comes out of the solution of the hydrodynamic equations. Here f is the distribution function which – including viscous corrections – can be written as [32, 39]

$$f = f_0 \left(1 + \frac{p_\mu p_\nu \Pi^{\mu\nu}}{2T^2(\epsilon + p)}\right), \tag{30}$$

where for simplicity we take the equilibrium distribution f_0 to be given by the Boltzmann-distribution[5] $f_0(x) = \exp(-x)$.

Furthermore, $d\Sigma^\mu$ is the normal vector on the freeze-out surface, parametrized as $d\Sigma^\mu = \left(\cosh\eta, \cos\phi\frac{d\tau_f(r)}{dr}, \sin\phi\frac{d\tau_f(r)}{dr}, \sinh\eta\right) r dr \tau_f(r) d\phi d\eta$ in our choice of coordinates [37]. Here $\tau_f(r)$ is the freeze-out time parametrized as a function of r or – put differently – the time at which the slab of matter at radius r has reached the freeze-out condition.

For this exploratory study, we will apply the Cooper-Frye freeze-out prescription to convert the hydrodynamic variables at a single specific temperature (the freeze-out temperature T_f) into transverse momentum spectra for particles. This is what also has been used in early ideal hydrodynamic calculations [61, 62]. Since we use a gluonic equation of state and do not include a realistic matching to hadronic degrees of freedom, we contend ourselves to study the effects of viscosity on the spectrum of gluons mostly.

For the spectrum, in terms of particle transverse momentum $p_\perp$, angle ϕ_p and rapidity y one thus finds

$$p_\mu d\Sigma^\mu = \left(m_\perp \cosh(\eta - y) - p_\perp \cos(\phi - \phi_p)\frac{d\tau_f(r)}{dr}\right)\tau_f(r) r dr d\phi d\eta, \tag{31}$$

with $m_\perp = \sqrt{p_\perp^2 + m_0^2}$ and m_0 the rest mass of the particle.

Since in our calculations we are only including transverse flow we have

$$p_\mu u^\mu = (m_\perp \cosh(\eta - y) u^\tau - p_\perp \cos(\phi - \phi_p) u^r), \tag{32}$$

---

[5] It is easy to change this to Bose-Einstein or Fermi-Dirac distributions, but for massive particles we have found the differences in resulting observables to be minimal.
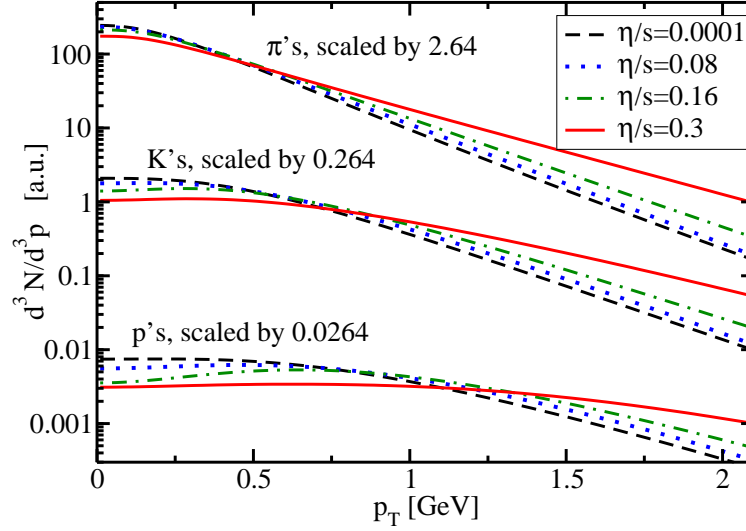
FIG. 6: Mass dependence of viscous effects: shown are spectra for pions, kaons and protons for a freeze-out temperature of $T_f = 0.135$ GeV and for $T_0 = 0.36$ GeV and $\Pi^{\mu\nu} = 0$ at $\tau_0 = 1$ fm/c. As can be seen, the higher the mass of the particle, the stronger do viscous effects change its low $p_\perp$ behavior.

which allows us to integrate out both angles ϕ and rapidities η in Eq.(29). Using

$$\int_{-\infty}^{\infty} d\eta \cosh^n \eta \exp(-x \cosh \eta) = \left(-\frac{d}{dx}\right)^n 2K_0(x),$$

$$\int_0^\pi \frac{d\phi}{\pi} \cos n\phi \exp(x \cos \phi) = I_n(x), \tag{33}$$

where $K_n(x)$ and $I_n(x)$ are modified Bessel functions one finds for the particle spectrum

$$E\frac{d^3N}{d^3p} = E\frac{d^3N_0}{d^3p} + E\frac{d^3\delta N}{d^3p}, \tag{34}$$

with the equilibrium part taking the form

$$E\frac{d^3N_0}{d^3p} = \frac{2d}{(2\pi)^2} \int r dr \tau_f(r) \left[m_\perp I_0(u^r p_\perp/T) K_1(u^\tau m_\perp/T) - \frac{d\tau_f(r)}{dr} p_\perp I_1(u^r p_\perp/T) K_0(u^\tau m_\perp/T) \right], \tag{35}$$

where the integral over r runs from 0 to the maximum freeze-out radius if $\tau_f(r)$ is a single-valued function (else one has to introduce a different parametrization of the freeze-out surface). Noting that the Bessel K functions always have the argument $u^\tau m_\perp/T$ (and similarly for the I's) we refrain from writing the argument in the following. Noting that

$$p_\mu p_\nu \Pi^{\mu\nu} = \Pi_r^r \left[2v m_\perp p_\perp \cosh(y - \eta) \cos(\phi_p - \phi) - p_\perp^2 \cos(2(\phi_p - \phi)) \right.$$
$$\left. - v^2 m_\perp^2 \cosh^2(y - \eta) - v^2 p_\perp^2 \sin^2(\phi_p - \phi) \right]$$
$$+ \Pi_\eta^\eta \left[-m_\perp^2 \sinh^2(y - \eta) + p_\perp^2 \sin^2(\phi_p - \phi) \right], \tag{36}$$

we then find the for the dissipative corrections to the spectrum

$$E\frac{d^3\delta N}{d^3p} = \frac{d}{(2\pi)^2} \int r dr \frac{\tau_f(r)}{2T^2(\epsilon + p)} \left\{ 2p_\perp m_\perp v \Pi_r^r \left[m_\perp (K_0 + K_2) I_1 - p_\perp \frac{d\tau_f}{dr} K_1 (I_2 + I_0) \right] \right.$$

$$-p_\perp^2 \Pi_r^r \left[2m_\perp K_1 I_2 - p_\perp \frac{d\tau_f}{dr} K_0 (I_3 + I_1) \right]$$

$$-v^2 m_\perp^2 \Pi_r^r \left[\frac{1}{2} m_\perp (3K_1 + K_3) I_0 - p_\perp \frac{d\tau_f}{dr} (K_0 + K_2) I_1 \right]$$

$$-v^2 p_\perp^2 \Pi_r^r \left[m_\perp K_1 (I_0 - I_2) - p_\perp \frac{d\tau_f}{dr} K_0 \frac{1}{2} (I_1 - I_3) \right]$$

$$+p_\perp^2 \Pi_\eta^\eta \left[m_\perp K_1 (I_0 - I_2) - p_\perp \frac{d\tau_f}{dr} K_0 \frac{1}{2} (I_1 - I_3) \right]$$

$$-m_\perp^2 \Pi_\eta^\eta \left[m_\perp \frac{1}{2} (K_3 - K_1) I_0 - p_\perp \frac{d\tau_f}{dr} (K_2 - K_0) I_1 \right] \Bigg\} , \tag{37}$$

where we remind that $v = u^r / u^\tau$.

In Fig.5, we show the inverse slope parameter $T_{\rm slope}$ of gluons which we define by calculating the gluonic spectrum at $T_f = 0.135$ GeV and fitting it by

$$E \frac{d^3N}{d^3p} \sim \frac{1}{T_{\rm slope}^2} \exp\left[-p_\perp / T_{\rm slope} \right]$$

for $0.2 < p_\perp < 1$ GeV (c.f.[63]). In Fig.5(a), the slope has been calculated for $T_0 = 0.36$ GeV, $\tau = 1$ fm/c and for the two extreme cases $\Pi^{\mu\nu}(\tau_0) = 0$ (full line) and zero initial longitudinal pressure Eq.(28) (dashed line). As can be seen from this figure, increasing η/s and leaving all other parameters unchanged leads to an increasing $T_{\rm slope}$ ("flatter spectra") for gluons, with no dramatic difference between the two different initial choices for $\Pi^{\mu\nu}$. However, as has been anticipated from our earlier studies neglecting the effect of transverse flow [39], one can compensate this effect by changing the effective initial conditions. This can be seen in Fig.5(b), where we show the spectral slope for the same freeze-out temperature, but different initial temperatures T_0.

It is also interesting to study how the presence of viscosity affects massive particles. To this end, hypothetical spectra of pions, kaons and protons for $T_f = 0.135$ GeV, $T_0 = 0.36$ GeV and $\Pi^{\mu\nu}(\tau_0) = 0$ at $\tau_0 = 1$ fm/c are shown in Fig.6. These spectra cannot be directly interpreted as real particle spectra because a realistic matching to a hadronic equation of state and the effects from higher mass resonance decays [64] are missing in this study[6]. Nevertheless, from Fig.6 one can glean that the more massive a particle is, the more viscosity affects its spectrum, in particular at low $p_\perp$. Indeed, this can be traced back to Eqs.(35,37) which in the limit of vanishing $p_\perp$ and neglecting radial dynamics ($v = 0$) predict negative d^3N/d^3p for large m_0/T, more specifically for

$$\frac{m_0}{T} > \frac{2(\epsilon + p) - \frac{15}{8} \Pi_\eta^\eta}{\Pi_\eta^\eta}. \tag{38}$$

Thus it seems that – whenever $\Pi_\eta^\eta / (\epsilon + p)$ becomes non-negligible – viscous corrections δN to the spectrum of high-mass particles become very large, e.g. more than 100 percent at low $p_\perp$. While it is unclear at which value of η/s this starts to be a problem in practice, it nevertheless serves as an indication that the assumption of small deviations from equilibrium [39] is breaking down. Consequently, the reliability of the tool we have used to probe the system dynamics, namely viscous hydrodynamics, becomes questionable. Thus, for η/s larger than a critical value, one probably has to use a different model than hydrodynamics to correctly calculate observables that are to be compared to experiments.

---

[6] See however [65] for a comparison to experimental data.

V.   CONCLUSIONS

We have studied the effect of shear viscosity in a hydrodynamic description of central heavy-ion collisions. We presented a simple algorithm to solve the relevant equations numerically and have successfully carried out several tests on this algorithm. These tests are not specific to our algorithm, but can in general be used to test any algorithm for solving relativistic viscous hydrodynamics. Assuming an ideal equation of state $\epsilon = 3p$ for simplicity we calculated the time evolution of the temperature profile of a central heavy-ion collision, finding that while viscous hydrodynamics in general cools slower, certain regions at later times may cool faster than in a corresponding ideal hydrodynamic calculation.

We also calculated the effect of viscosity on the slope of gluon spectra, finding that for small values of η/s, changes can largely be compensated by lowering the temperature at which the hydrodynamic evolution is started. For massive particles we find that viscosity changes the spectrum the more the higher the mass of the particle under consideration. We give arguments that for a sufficiently large value of η/s, corrections which in the derivation of the viscous hydrodynamic equations had been assumed to be small actually become large, thus signaling the possible breakdown of any hydrodynamic description of the system.

Even though our simplifying assumptions (ideal equation of state, no feed-down correction, only radial flow) leave ample room for improvement, we hope that our study provides the basis for coming viscous hydrodynamic algorithms as well as fits to experimental data.

Acknowledgments

[1] D. Teaney, J. Lauret and E. V. Shuryak, Phys. Rev. Lett. **86** (2001) 4783.
[2] P. Huovinen, P. F. Kolb, U. W. Heinz, P. V. Ruuskanen and S. A. Voloshin, Phys. Lett. B **503** (2001) 58.
[3] P. F. Kolb, U. W. Heinz, P. Huovinen, K. J. Eskola and K. Tuominen, Nucl. Phys. A **696** (2001) 197.
[4] T. Hirano and K. Tsuda, Phys. Rev. C **66**, 054905 (2002).
[5] P. F. Kolb and R. Rapp, Phys. Rev. C **67**, 044903 (2003).
[6] K. Adcox *et al.* [PHENIX Collaboration], Nucl. Phys. A **757** (2005) 184.
[7] B. B. Back *et al.* [PHOBOS Collaboration], Nucl. Phys. A **757** (2005) 28.
[8] I. Arsene *et al.* [BRAHMS Collaboration], Nucl. Phys. A **757** (2005) 1.
[9] J. Adams *et al.* [STAR Collaboration], Nucl. Phys. A **757** (2005) 102.
[10] P. Arnold, G. D. Moore and L. G. Yaffe, JHEP **0011** (2000) 001.
[11] P. Arnold, G. D. Moore and L. G. Yaffe, JHEP **0305** (2003) 051.
[12] P. Kovtun, D. T. Son and A. O. Starinets, Phys. Rev. Lett. **94** (2005) 111601.
[13] R. A. Janik, Phys. Rev. Lett. **98** (2007) 022302.
[14] E. V. Shuryak, Nucl. Phys. A **750** (2005) 64.
[15] T. D. Lee, Nucl. Phys. A **750** (2005) 1.
[16] M. Gyulassy and L. McLerran, Nucl. Phys. A **750** (2005) 30.
[17] U. W. Heinz, arXiv:nucl-th/0512051; Nucl. Phys. A **721** (2003) 30.
[18] B. Muller and J. L. Nagle, arXiv:nucl-th/0602029.
[19] S. K. Blau, Phys. Today **58N5** (2005) 23.

[20] M. Riordan and W. A. Zajc, Sci. Am. **294N5** (2006) 24.

[21] I. R. Klebanov, arXiv:hep-th/0009139.

[22] F. Karsch and H. W. Wyld, Phys. Rev. D **35** (1987) 2518.

[23] A. Nakamura and S. Sakai, Phys. Rev. Lett. **94** (2005) 072305.

[24] S. Mrowczynski, Acta Phys. Polon. B **37** (2006) 427.

[25] P. Arnold and G. D. Moore, Phys. Rev. D **73** (2006) 025006.

[26] P. Arnold and G. D. Moore, Phys. Rev. D **73** (2006) 025013.

[27] M. Asakawa, S. A. Bass and B. Muller, Phys. Rev. Lett. **96** (2006) 252301.

[28] M. Asakawa, S. A. Bass and B. Muller, Prog. Theor. Phys. **116** (2007) 725.

[29] E. Iancu and R. Venugopalan, arXiv:hep-ph/0303204.

[30] P. Romatschke and R. Venugopalan, Phys. Rev. Lett. **96** (2006) 062302.

[31] P. Romatschke and A. Rebhan, Phys. Rev. Lett. **97** (2006) 252301.

[32] D. Teaney, Phys. Rev. C **68** (2003) 034913.

[33] W.A. Hiscock and L. Lindblom, Phys. Rev. D **31**, 725 (1985).

[34] W. Israel, Ann.Phys. **100** (1976) 310; W. Israel and J.M. Stewart, Phys. Lett. **58A** (1976) 213; W. Israel and J.M. Stewart, Ann.Phys. **118**, (1979) 341.

[35] M. Prakash, M. Prakash, R. Venugopalan and G. Welke, Phys. Rept. **227** (1993) 321.

[36] A. Muronga, Phys. Rev. Lett. **88** (2002) 062302 [Erratum-ibid. **89** (2002) 159901]; Phys. Rev. C **69** (2004) 034903.

[37] A. Muronga and D. H. Rischke, arXiv:nucl-th/0407114.

[38] A. K. Chaudhuri and U. W. Heinz, J. Phys. Conf. Ser. **50** (2006) 251; U. W. Heinz, H. Song and A. K. Chaudhuri, Phys. Rev. C **73** (2006) 034904.

[39] R. Baier, P. Romatschke and U. A. Wiedemann, Phys. Rev. C **73** (2006) 064903.

[40] R. Baier, P. Romatschke and U. A. Wiedemann, Nucl. Phys. A **782** (2007) 313.

[41] K. Tsumura, T. Kunihiro and K. Ohnishi, arXiv:hep-ph/0609056.

[42] T. Koide, G. S. Denicol, Ph. Mota and T. Kodama, arXiv:hep-ph/0609117.

[43] P. J. E. Peebles and J. T. Yu, Astrophys. J. **162** (1970) 815.

[44] D. N. Spergel *et al.*, arXiv:astro-ph/0603449.

[45] V. Mukhanov, "Physical foundations of cosmology", Cambridge (U.K.) University Press (2005).

[46] G. Baym, B. L. Friman, J. P. Blaizot, M. Soyeur and W. Czyz, Nucl. Phys. A **407** (1983) 541.

[47] Y. Lallouet, D. Davesne and C. Pujol, Phys. Rev. C **67** (2003) 057901.

[48] J. Casalderrey-Solana, E. V. Shuryak and D. Teaney, J. Phys. Conf. Ser. **27** (2005) 22 [Nucl. Phys. A **774** (2006) 577].

[49] L.P. Kadanoff and P.C. Martin, Ann.Phys.(N.Y.) **24**, 419 (1963).

[50] S. Gavin and M. Abdel-Aziz, Phys. Rev. Lett. **97** (2006) 162302.

[51] L. D. McLerran and R. Venugopalan, Phys. Rev. D **49** (1994) 2233; *ibid.*, 3352.

[52] A. Krasnitz and R. Venugopalan, Phys. Rev. Lett. **84** (2000) 4309.

[53] T. Lappi, Phys. Rev. C **67** (2003) 054903.

[54] F. Gelis and R. Venugopalan, Nucl. Phys. A **776** (2006) 135.

[55] F. Gelis and R. Venugopalan, Nucl. Phys. A **779** (2006) 177.

[56] P. Romatschke and R. Venugopalan, Phys. Rev. D **74** (2006) 045011.

[57] K. Fukushima, F. Gelis and L. McLerran, arXiv:hep-ph/0610416.

[58] D. A. Teaney, J. Phys. G **30** (2004) S1247.

[59] A. K. Chaudhuri, Phys. Rev. C **74** (2006) 044904.

[60] F. Cooper and G. Frye, Phys. Rev. D **10**, 186 (1974).

[61] H. Von Gersdorff, L. D. McLerran, M. Kataja and P. V. Ruuskanen, Phys. Rev. D **34** (1986) 794.

[62] L. D. McLerran, M. Kataja, P. V. Ruuskanen and H. von Gersdorff, Phys. Rev. D **34** (1986) 2755.

[63] S. S. Adler *et al.* [PHENIX Collaboration], Phys. Rev. C **69** (2004) 034909.

[64] E. Schnedermann, J. Sollfrank and U. W. Heinz, Phys. Rev. C **48** (1993) 2462.

[65] P. Romatschke, arXiv:nucl-th/0701032.